

Towards Energy Efficient Machining of Titanium Alloy – Ti6Al4V: Characterising Chip Morphological Impact on Specific Energy Use During the Mechanical Finish Cutting Process

Nicholas Tayisepi

Department of Industrial and Manufacturing Engineering
National University of Science and Technology
Gwanda Road/Cecil Avenue, P. O. Box AC 939, Ascot, Bulawayo, ZIMBABWE
nicholas.tayisepi@nust.ac.zw

ABSTRACT

During mechanical cutting of aircraft grade titanium alloy, Ti6Al4V, chip morphology features observation relay fundamental intelligence towards understanding the machining activity energy efficiency management. In the present study, the effect of chip formation, on specific energy use, was experimentally investigated. Design of experiments was used to plan the 18 machining experiments iteration set in Minitab 22 software. The input cutting parameters were varied and the segmented chip morphological variation was studied in order to understand its effect on the energy efficiency, which is reflected through specific energy use. Key, Ti6Al4V material chip formation feature attributes, were examined and characterised as regards how the chip profile features correlate with specific energy use during cylindrical billet exterior cutting on the CNC turning machine tool. The research, aimed to generate insight into the energy efficient machining of the Ti6Al4V, as mirrored through the chip morphology system. Furthermore, the intention was to get a macroscopic insight about the energy use from observing the chip profile trends during machining of the high grade titanium alloy. Results established the correlation between the seven analysed chip morphology attributes changes with specific energy use minimisation up to some point beyond which the reduction trend changes direction towards energy consumption increase. The profiles of the chip morphology versus specific cutting energy plot suggest the subsistence of an energy use optimum point during the cutting of Ti6AL4V. The study findings provide important reliable guidance to the machining industry stakeholders who could apply this knowledge to monitor the process efficiency of their operations by macroscopically monitoring the features of the cutting chips produced. Conclusion reached is that it is feasible to observe the specific energy use trend, of the machining process, through observing the chip morphology system. Future work relate to establishing the optimum operating parameters from the chip morphology models.

Keywords

Energy efficiency, chip morphology, specific cutting energy, machining process, titanium alloy

INTRODUCTION

Titanium alloys have seen increased demand in various industries such as the aerospace industry and the bio-medical field in recent years. This is due to its superior properties such as excellent strength-to-weight ratio, strong corrosion resistance and ability to retain high strength at elevated temperature (Boyer, 1996; Ezugwu, et al., 2003). This demand has resulted in the requirement to increase machining speed and consequently the material removal rate. This has presented several challenges due to the intrinsic difficulties of the machinability of the Ti6Al4V material. Hence, extensive studies currently surrounding the expanded use and processing of the material. This current work seeks to characterise the interaction of the material chip morphological features with the process level energy use during its machining. Energy Efficiency gives prominence to the relationship between the amounts of energy resources deployed for a task as compared to the output achieved from the activity (ISO 9000:200, 2000). Generally, it compares the relationship between the output realised and the input resources used. Measures to analyse the energy efficiency, of machine tools in use, have been developed and deployed. Energy efficiency can be specified using a variety of indicators or measures based on physical or economic parameters. Specific cutting energy consumption (SEC) is one of the most widely accepted measures in industry and by researchers (Tao & Xun, 2013), to explain the machining energy efficiency or the machining process energy efficiency. Through it, values of energy consumption of the machining process can be accurately predicted. SEC is the amount of energy required to remove a unit volume or mass of material, and it reflects the energy efficiency of the machining process. According to Zhou et al (2016), SEC provides the mapping relationship between the processing parameters and the energy use. Neugebauer et al (2011) and Kalpakjian and Schmidt (2009), explained that during machining, due to the mechanical losses in the machine power train, drive and actuation systems the

power and energy (E_{mc}) which is required for the actual operation of the machine tool is greater than the power and energy (E_{pr}) required to drive the cutting process and material separation (Neugebauer, et al., 2011; Kalpakjian & Schmidt, 2009). Thus, according to this reasoning, energy efficiency represents the machining and process energy ratios. It is essential to analyse and understand the cutting process from a specific cutting energy use-based-processing signature perspective as a platform for improving the machining process performance of Ti-alloys.

Efficient metal material machining requires access to data relating the machining parameters to the work material for a given process (ASM International, 1988). The important process assessment parameters, during machining, include: tool life, cutting forces, chip formation, surface finish, power consumption requirements and cutting temperature and fluids. This research focuses on the influence of chip morphology on specific energy consumption during the turning process of Titanium alloy Ti6Al4V. Many authors have studied chip morphology and characterised it against cutting parameters mainly (Vyas & Shaw, 1999; Oosthuizen, et al., 2013). However, there is hardly much publications linking chip morphology with machining energy use expressed independently of the cutting parameters. An evaluation the chip morphology parameters formation - during the machining operation - allows information to understanding the adequacy of the cutting conditions used, towards the cutting process stability and energy use efficiency. Thus, this research set out to experimentally study the effects of chip morphology on specific energy use, at process level, during the machining of grade 5 titanium alloy. The data adduced was used to extract the link between chip morphology and specific cutting energy (SEC) independently from the changes in cutting parameters that would be used to produce the variation in chip morphology. The aim is to characterise the variation of energy use trends with the changing profile of the material chip so that it becomes feasible to monitor the machining energy use trend through observing the chip

morphology without having to resort to physically measuring the chip parameters or online energy measurements all the time. The research intended to tackle the challenges of energy optimisation in production systems by experimentally investigating the influence of chip formation on the energy consumption during the machining of Ti6Al4V. The energy consumed during a machining operation can be segmented into different functional activities (Dahmus & Gutowski, 2004; Rajemi & Mativenga, 2008; Rajemi, et al., 2009; Gutowski, et al., 2006). The machining energy refer to the amount of energy required to remove the workpiece component material under different process conditions. Broadly the required power, for a given machine tool, is composed of the constant and the variable energy components (Dahmus & Gutowski, 2004; Guo, et al., 2012). The constant power component relate to the power assigned to the machine tool accessories such as the computer, pumps, fans and lighting. This power is not influenced by the machining parameter settings as the variable power is. Variable power depends on the process parameters and is mainly attributed to the spindle and axes drives (Guo, et al., 2012), under the cutting resistance load. The total power required for the machining operation is, thus, a sum of the constant power and the variable power. It is, thus, vital to assess the machining process utilising an energy-based processing signature methodology with the intent of enhancing the machining energy and cost performance.

1.1 Metrics of Machining Energy Efficiency

Different measures are used to determine machining energy efficiency. Sebastian (2012) and Zhou et al, (2016) proposed an energy efficiency definition of the machine tool based on the power demand, wherein they compared the production output to the energy factored into the process. Instantaneous energy efficiency and process energy are the two modes into which Liu et al partitioned machine tools energy efficiency (Liu, et al., 2013). The

ratio of material removal cutting power $P_{cut}(t)$ and the machine input power $P(t)$ is called machine instantaneous energy efficiency $\eta_{energy}(t)$. The process energy efficiency (η_{energy}) is expressed as the ratio of the effective energy and the energy consumed by the system in a processing time (T) in the integral form. This is mathematically presented in equation 1.

$$\eta_{energy} = \frac{E_{cut}}{E} = \frac{\int_0^T P_{cut}(t)dt}{\int_0^T P(t)dt} \quad [1]$$

One other, of the most commonly accepted, measures of energy efficiency presently used by the manufacturing industry is specific cutting energy consumption (SEC) (Tao & Xun, 2013; Zhou, et al., 2016). During machining the energy consumption may be evaluated through consideration of the specific cutting energy (J/mm^3). This is used to express the machining process or machine energy efficiency. The specific cutting energy consumption is defined as the energy required to remove unit volume or mass of material (Zhou, et al., 2016). In some studies SEC is called energy intensity or specific cutting energy. SEC are categorised as: *Direct specific cutting energy for material removal (SEP, μ_1)* – computed through dividing the variable power, used for the actual machining, by the material removal rate. This explains the process level energy actually used to physically form the chip as the material is being removed, i.e, the energy per unit volume (Guo, et al., 2012; Anderberg, et al., 2012; Zhou, et al., 2016). SEP data can be computed analytically or measured practically Else this data can be read off handbooks. The SEP considers the specific cutting energy related to the machining activities without giving regard to the non-material removing activities of the machine (i.e. when MRR = 0). Thus, it makes the formula a suitable measure when there is need to comparing different operations against each other; *Specific cutting energy based on total power required to run the whole machine system (SET, μ_2)* - computed as the ratio of the total machine power to the rate of material

removal (MRR). This refers to the total energy that must be fed to the machine in order to remove material (Liu, et al., 2013). This yields the most comprehensive value of the effective specific cutting energy used by the machine tool. This value will include also the energy contribution of the auxiliary (non-cutting) functions like coolant pump driving, spindle start, tool repositioning, axes jogging, entering and exiting cut inter alia activities. This specific cutting energy value would alternatively be expressed as as the ratio of the energy used in joules to the volume of material removed (mm^3) per given time interval (MRR); Specific cutting energy based on several units of production to be considered (μ_3) - Where several units of production have to be considered, the total energy can be compared to the total volume of material removed to get the specific cutting energy (μ_3) (Zhou, et al., 2016). The value (μ_3) expresses the energy efficiency of the entire machining process. It also includes all non-value adding machining activities which consume energy (like rapid traverse) necessary to machine the component, energy for keeping the machine in standby mode or other non-cutting machining status; *Specific cutting energy based only on fit-for-use parts* (μ_4) - in production all the machined parts are categorised as qualified (good and fit for use) parts, defective parts and scrapped parts. Defective or scrapped parts may require rework, further processing or disposal. This mean that additional work may be required. Thus, only qualified parts should be considered in order to effectively compute the specific cutting energy (μ_4).

From the foregoing it is apparent that energy consumption is significantly affected by changing the machining conditions. SEC expresses energy efficiency from the perspective of the effective machine input and output power or energy. The value of SEC is used to estimate the energy use levels of the machining process and its value is affected by the machine load (Zhou, et al., 2016). SEC covers the mapping relationship between energy consumption and the material removal rate - MRR (Liu, et al., 2013). Its value can be used to compare

the energy efficiency differences of a machining process under different processing parameters and can be used to reflect the energy intensity and the productivity differences in distinct machining processes. Thus, the total specific cutting energy (SET) is the sum of the specific process energy (SEP) and the specific constant energy (SCE) (Diaz , et al., 2009). The specific constant energy (SCE) is computed as the ratio of constant power to the material removal rate. Specific power (P_{SEP}) and material removal rate can be used to estimate the main cutting force (F_c). The total horsepower P is given by Paul (2007) as the product of the specific power and the material removal rate. The third measure of efficiency is termed machining efficiency, wherein, it is determined as a ratio of the mechanical powers. Some studies define machine efficiency - η - (or mechanical efficiency) as the ratio of output power (P_{out}) to input power (P) of the machine (Zhou, et al., 2016). The challenge with η is that it does not show how the power or energy is used to exactly cut (Zhou, et al., 2016). Both η and $\eta_{efficiency}$ denote the input to output energy relationships. Energy efficiency is much more encompassing than mechanical efficiency. In essence η is included in, and is a component, $\eta_{efficiency}$. η reflects the effect of the mechanical energy losses and electrical losses whereas, $\eta_{efficiency}$ include all kinds of energy loss. When $\eta_{efficiency}$ is combined with production it reflect the relationship between energy input and product output. Thus, the use of SEC to express energy efficiency of the machine also reflects how the machining energy is distributed and used to remove material in detail (Draganescu, et al., 2003).

In this research write-up, μ_1 was selected for use, as the specific cutting energy consumption measure. This was considered representative of the true value of specific cutting energy use in energy-efficient machining, considering energy use as affected by the variable process parameters. However, it is pertinent to determine how exactly this energy consumption can integrally be physically

interpreted through the morphological profile of the chips removed.

1.2 Mechanical Energy and Chip Formation Issues In Metal Machining

Cutting is a process of high localised stresses and extensive plastic deformation and shearing, in which the high compressive and frictional contact stresses on the cutting tool, result in the various cutting forces. The specific cutting energy required to produce the chip is a function of the mechanical energy to produce shear in the work piece and the frictional energies consumed by the chip tool interaction on rake and flank faces of the tool (Oosthuizen, et al., 2013). During this transformation a significant fraction of the energy in the form of heat is transferred to the chip and tool from the shear-plane and tool-chip interface respectively. This interaction between the cutting tool and work piece at different cutting conditions also affects chip formation, surface quality of the work piece and tool wear. Intrinsic characteristics and processing conditions affect energy efficiency on machine tools. The details of the intrinsic characteristics affecting the energy efficiency losses are shown on Figure 1.1 and these are factors such as motor loss, hydraulic loss and mechanical system loss. The reactive power losses tend to dominate influencing the energy efficiency (Zhou, et al., 2016).

At the cutting zone as the tool penetrates the cut material, energy is concentrated in the primary and secondary shear zone. Material entering the cutting zone experiences shear deformation at the primary deformation zone. High strain and great-rate shear flow occur in this zone with moderate temperature. Where material is separated by the cutting action at the cutting zone the energy expended is decomposed into two major components of shear energy and friction energy (Ma, et al., 2014). The shear energy is the useful function, whereas, friction energy is waste from the cutting process. The material being removed is separated along the cutting edge in the form of chips which take different forms. Energy is expended in this zone to remove material. Post the primary shear zone, the chip flows round the cutting

edge and slides along the rake face of the cutting tool forming the secondary shear zone. This zone is characterised by intense friction and shear at the tool-chip interface under high temperature (Hua & Shivpuri, 2004). Energy at this zone is absorbed in overcoming friction (Ma, et al., 2014), and is not considered useful work. Thus, in this consideration the energy efficiency at material removal process level is defined as the ratio of the shear energy to the total cutting energy. The mathematical relationships is outlined in equation 2.

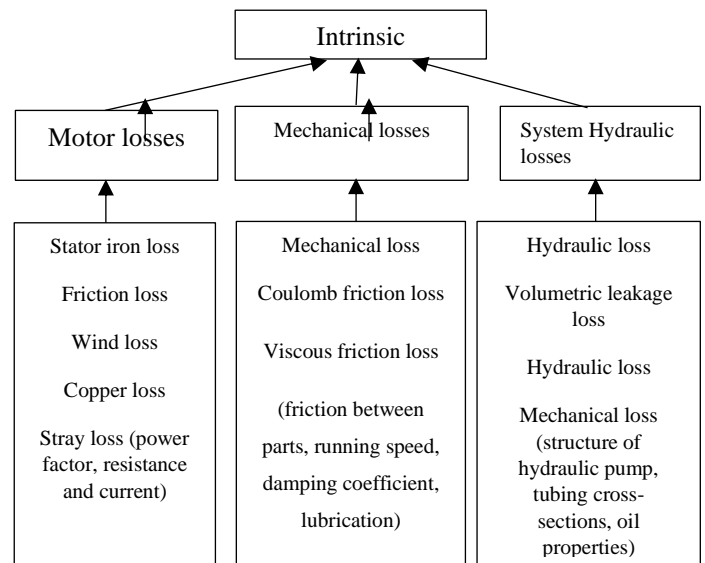


Figure 1.1 Intrinsic characteristics and processing conditions which affect energy efficiency on the machine tool (Courtesy: (Zhou, et al., 2016))

The total cutting mechanical energy used in machining is defined by (Ma, et al., 2014):

$$U_c = F_c V = U_s + U_f \quad [2]$$

Where, F_c is the cutting force and V is the cutting speed, U_c is the sum of shear, U_s and friction energy, U_f .

1.3 Titanium Alloy and Its Application Properties and Environments of Use

Titanium alloys are considered a viable material in many engineering applications due to the material's attractive properties as compared to other engineering materials. They have outstanding high hot strength (retains strength at high temperatures) especially Ti-6Al-4V, high

chemical inertness, and superb resistance to corrosion and generally very strong. Furthermore, Ti-alloys offer favourable mechanical characteristics such as toughness and tenacity (Calamaz, et al., 2008). The hypoallergenic properties of titanium, as it is nickel-free, makes it medically compatible - bio-compatibility (Repro, 2002; Ozel & Ulutan, 2012). Ti6Al4V bio-compatibility properties see it used in medical field applications. Ti-alloys unique combination of mechanical and physical properties have made them desirable to a wide variety of industrial applications (Annamarie, 2004). They are applied in the reliability demanding industries such as the aerospace, chemical and energy industrial sectors, for automotive and industrial machinery components, to electronics, offshore oil drill rigs, shipbuilding (especially submarines) and sea water desalination plants, and consumer goods, heat exchangers, petrochemical plants and medical devices (Jawahir, et al., 2011; Oosthuizen, et al., 2010; Ozel & Ulutan, 2012; Machado & Wallbank, 1989; Boyer, 1996; Ezugwu, et al., 2003). The exceptional elevated temperature performance, added with corrosion resistance sees Ti6Al4V alloys mainly applied in the aviation industry most significantly in jet engines and airframe components that are subject to temperatures up to 1100° F and for other structural parts. Usage is significant in commercial and military aircraft. Ti6Al4V alloys is also an excellent and attractive material due to its combination of high specific strength (strength-to-density ratio) and fracture resistance characteristics and it also finds increasing usage in the nuclear industries (Sun & Guo, 2008).

Relating to the general physical and mechanical properties of Ti6Al4V, titanium alloys are mainly classified according to their microstructural arrangements and alloying elements. They fall into four (4) major categories viz pure unalloyed titanium, alpha (α) phase titanium, alpha beta ($\alpha\beta$) and beta (β) phase titanium. The alpha (α) phase titanium has a hexagonal close-packed crystalline structure [hcp] whilst beta (β) phase has a body-centred cubic crystalline structure [bcc]. The

Ti6Al4V used in this research is an alpha-beta alloy. The alpha phase proportion in the Ti6Al4V alloy, according to Dabrowski varies from 60 to 90% (Dabrowski, 2011). Pure titanium is allotropic behaviourally, i.e. it undergoes a reversible crystal structure transformation from the hexagonal close-packed alpha structure to the body-centred cubic structure at temperatures beyond 882.5 °C (1,620°F). Below this temperature from ambient temperature the material remains stable in the alpha phase (Ezugwu & Wang, 1997; Collogs, 1983; Dabrowski, 2011). The body-centred cubic structure beta phase in the pure titanium remains stable from approximately 882.5 °C (1620°F) to the melting temperature point at approximately 1604 °C (3040°F) (Dabrowski, 2011). The crystalline structure transition temperature is strongly influenced by the addition of alloying elements to the titanium. Materials such as aluminium (Al), oxygen (O), nitrogen (N) and carbon (C) tend to raise the beta-transus temperature as they stabilise the alpha phase in the material. On the other hand alloying elements such as vanadium (V), tungsten (W), chromium (Cr), copper (Cu), iron (Fe), manganese (Mn), molybdenum (Mo), columbium (Nb) and silicon (Si) stabilises the beta phase by decreasing the transformation temperature from alpha to beta (Collogs, 1983; Dabrowski, 2011; Ribeiro, et al., 2003). Heat treatment and addition of alloying elements to titanium alters its microstructure and properties. Thus, providing the wide range of the physical and mechanical properties of the material (Ribeiro, et al., 2003). The specific heat of Ti6Al4V increases with rising temperature from 565 J/Kg K at room temperature to 1060 J/Kg K at 980 °C. Its thermal conductivity also increases with increasing temperature, ranging from 6.6 W/mK at 20 °C to 21.5 W/mK at 1050 °C (Ozel & Ulutan, 2012). This low thermal conductivity against the huge temperature difference occurring at the cutting zone imply that most of the heat generated will accumulate at the tool tip. The coefficient of thermal expansion of Ti6Al4V insignificantly change and is almost constant ranging from $9.4 \times 10^{-6} \text{ K}^{-1}$ at room temperature to $1.07 \times 10^{-5} \text{ K}^{-1}$ at 1000 °C. It is apparent that

the Ti6Al4V alloy thermal conductivity ($K_{Ti} = 7.0 - 7.3 \text{ W/mK}$) by any means is very low as compared to that of steel ($K_{Steel} = 50.7 \text{ W/mK}$) (Ribeiroa, et al., 2003). Against the specific heat capacity high value of 560 it means that there is rapid heat build-up at the cutting zone. This possess potential threat to the component material and the cutting tool tip. Titanium alloys machining is characterised by the production of segmented chips for a wide range of cutting speeds and feeds (Cook, 1953; Calamaz, et al., 2008; Hou & Komanduri, 1995; Vyas & Shaw, 1999). Hou and Komanduri (1995), reported the critical cutting speed of 9 m/min for Ti-alloy being the lowest minimum cutting speed beyond which any machining of Ti6Al4V alloy tend to produce segmented chips as a result of the setting in, into the machining process, of thermoplastic instability.

1.0 EXPERIMENTAL SET-UP AND DESIGN

The purpose of the experimental study was to establish, if any, correlation can be deduced between chip morphology geometrical characteristics with energy use reduction of the machining process. Single-point orthogonal machining, in which the cutting tool has a plane face and a single straight cutting edge oriented perpendicular to the direction of motion – with a depth of cut smaller compared to the length of the tool cutting edge, was conducted. The machining experiments were conducted on the Efamatic CNC lathe (model: RT-20 S, Maximum spindle speed 6000 RPM) machine, under different cutting conditions. Chip morphology geometry and total and specific cutting energy were monitored and measured on the first pass (new tool) and last pass (worn tool) of each experimental iteration. The influence of chip formation on energy consumption of the machining process was analysed in order to establish the chip morphology profile form favouring energy use optimisation. A solid cemented carbide tipped tool (ISO code designated CNMX 12 04 A2-SM H13A with coating) in a Sandvik tool holder (DCLNL 2525 M12) was used for turning Ti6Al4V with conventional flood cooling. This tool, with chip breaking technology, is recommended for cutting Ti-

alloy by some researchers (Ribeiroa, et al., 2003) and is generally used in the industry (Oosthuizen, et al., 2010). The tool tip and the holder are shown on Figure 2. Further particulars of the tool are: positive rake angle 15° , -6° inclination angle and 45° entry angle. In order to conform with the ISO Standard 3685-1993 (E) for single point turning tools a wear criterion of flank wear, $V_B = 300 \mu\text{m}$ (Tayisepi, et al., 2016) was used for all the machining experiments.

The experimental material Ti6Al4V (Grade 5) titanium alloy was supplied in annealed condition at 36 HRC as a solid round bar ($\varnothing = 75.4 \text{ mm} \times 250 \text{ mm}$ long). The experimental parameters used and specimen mechanical strength characteristics (as per materials certificate) are presented in Tables 1 (a and b respectively).

Online power measurements were taken using a KYORITSU ELECTRICAL 3 PHASE DIGITAL POWER METER MODEL 6305 with the KEW POWER PLUS2 power signal recordings captured and read off an Acer Aspire 5551 Laptop running on Windows 7. The experimental set-up is shown in Figure 3.

2.1 Chip Morphology Parameters

Metallographic chip samples were collected, with the intention to characterise the cutting zone significant deformation process parameters on the chip, and analysed how these impact on the energy use efficiency, of the turning process of Ti6Al4V. Some of the chip parameters were measured, whilst some were derived from calculations, using geometrical relationships of the cutting condition parameters and the measured chip parameters. The chip deformation features: chip ratio, chip shear velocity, chip speed, deformation angle and segmentation frequency were calculated. Segmentation teeth pitch (P), on Figure 4, maximum chip thickness (peak height – T_p), minimum thickness (valley height – T_v) and the segmentation shear angle (θ) were measured using a stereo microscope. Segmentation or cracking (cycle) frequency (SF), is calculated from knowing the chip speed or shear plane speed, teeth



Figure 2: Turning tool holder and cutting tip used

Table 1: Experimental parameters and specimen mechanical properties

| (a) | | (b) | |
|--------------------------------|-----------------------|---|----------|
| Experimental Parameters | | Material properties for Ti6Al4V (Grade 5) | |
| Parameter | Condition | Ti6Al4V mechanical properties | |
| Cutting speed, $[v_c]$, m/min | 50, 70, 150, 200, 250 | Ultimate Tensile Strength [MPa] | 969 |
| Feed rate, $[f_n]$, mm/rev | 0.1, 0.2, 0.3 | 0.2% Yield Strength [MPa] | 847 |
| Depth of Cut, $[DoC]$, mm | 0.5 constant | Young's Modulus [GPa] | 115 |
| Coolant | Flood | Elongation [%] | 13 |
| | | Hardness [HRC] | 36 |
| | | Heat Treatment Condition | Annealed |

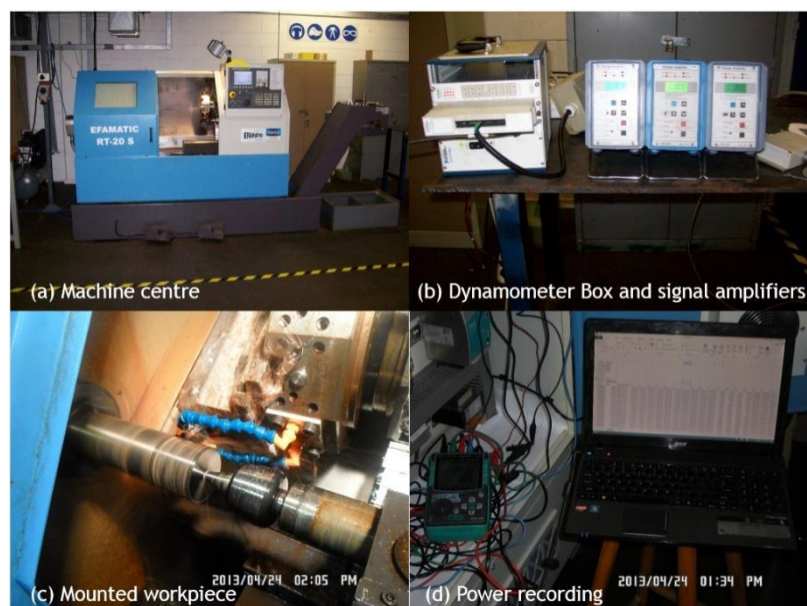


Figure 3: Experimental set-up

pitch (P) and the cutting speed (Miroslav , et al., 2013; Vyas & Shaw, 1999). Thus,

$$SF = v_{ch}/P \quad [3]$$

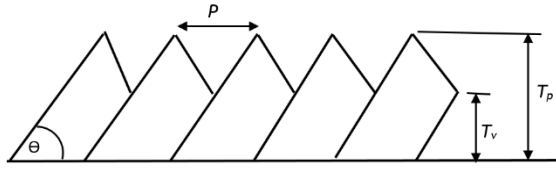


Figure 4: Segmented chip morphology parameters

Where v_{ch} is the chip velocity and P is the teeth pitch or segment length.

During the machining, of Ti6Al4V, the teeth peak height represents the maximum thickness portions of the chip teeth segments and the valley heights indicate the thickness of the continuous portions of the chip. The tooth height (T_h) indicates the portion between the peak (T_p) and valley (T_v) and this is the thickness of the separated portion of the chip. T_h is thus, computed as the difference between T_p and T_v . Hence;

$$T_h = T_p - T_v \quad [4]$$

The degree of segmentation (G), expresses the ratio of the tooth height to the peak height. It is calculated from (Upadhyay , et al., 2014):

$$G = (T_p - T_v)/T_p = T_h/T_p \quad [5]$$

The other parameters which are calculated include the following (Miroslav , et al., 2013; Upadhyay , et al., 2014):

(a) The cutting ratio, R is computed from:

$$R = T_p/T_v = v_{ch}/v \quad [6]$$

Where v_{ch} is the chip velocity (speed) and v is the cutting speed.

(b) The deformation angle, θ is determined from:

$$\theta = (\cos \gamma_n)/(R - \sin \gamma_n) \quad [7]$$

Where γ_n is the tool rake angle in degrees.

(c) The chip speed, v_{ch} can be derived from cutting speed thus:

$$v_{ch} = (v_c \sin \theta)/(\cos \theta - \gamma_n) \quad [8]$$

(d) Shear speed, v_{sh} can also be calculated from:

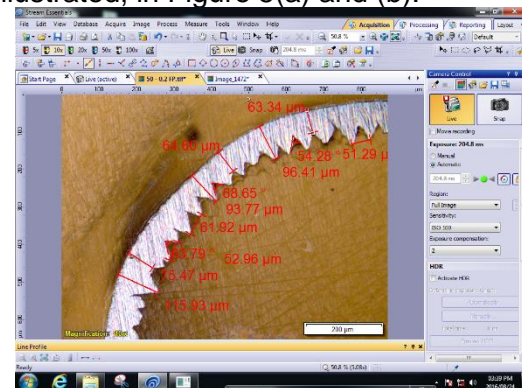
$$v_{sh} = (v_c \cos \gamma_n)/(\cos (\theta_1 - \gamma_n)) \quad [9]$$

(e) In similar way, chip deformation can be expressed as:

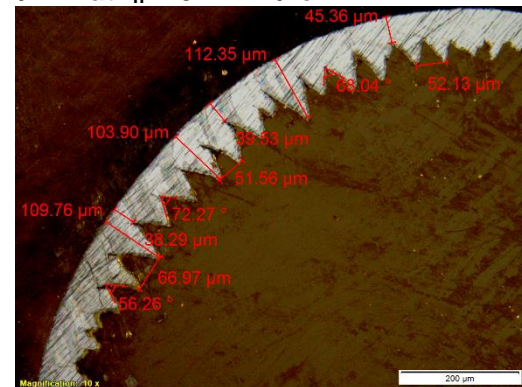
$$\gamma_{sh} = (\cos \gamma_n)/(\cos (\theta_1 - \gamma_n) \cdot \sin \theta_1) \quad [10]$$

Where γ_{sh} is the shear angle in degrees

During the experimental machining process, chips were collected for every first and last pass of an experiment iteration. Chips obtained after machining were mounted with Durofast epoxy resin so that they stood on their edge in order to make the cross-section visible after polishing straight across its length (Calamaz, et al., 2008). Chips were mounted, ground, polished and etched for morphology photographing, parameter measurements and analysis. A BX51M Olympus Optical Microscope was used to examine the chips. The chips were collected and analysed using the Olympus DP25 digital camera lens. The typical optical microscope visual screen images and the parameters measured, during the experimental process, are shown, illustrated, in Figure 5(a) and (b).



(a) image on computer screen – $v_c = 50$ m/min at $f_n = 0.2$ mm/rev



**(b) $v_c = 70$ m/min at $f_n = 0.2$ mm/rev
Figure 5. Chip morphology profile measured parameters on screen**

Qualitative and quantitative (whereby different physical parameters of the chips and energy used were measured) results of the analysis are presented on the outline ensuing.

3. RESULTS AND DISCUSSION

The ensuing sections provide results of the research under the sections thus:

3.1 Chip Formation

Chip morphology analysis provides an understanding of the cutting process and proffers information about suitable conditions to be used for the cutting process. Some of the chip morphology features were quantified by classical chip parameters computation (equations 3 - 10). This include such parameters as chip compression ratio, degree of segmentation, segmentation frequency and gradient of segmentation. Other parameters such as chip thickness, chip pitch, chip teeth peak and valley height were physically measured. Chips were collected, measured (with an optical microscope) and analysed for several parameters. As macroscopically viewed, the chip formation system was segmented. Table 2, presents summary of some of the experiment results with regards to total machining and specific cutting energy and the chip morphology parameters – chip width, segmentation teeth, pitch shear segmentation angle, degree of segmentation and shear segmentation frequency (Seg. Freq.) with variation of the cutting input parameters - cutting speed, v_c and feed rate, f_n .

Table 3 and Table 4, respectively, show the chip morphology at, respectively, varying cutting speeds at 0.3 mm/rev feed rate and at varying feed rates at a cutting speed of 150 m/min. It is apparent from the images that chip overall thickness tended to increase with the increase of feed rate, whereas it remains almost constant with the increase in cutting speed. The uncut chip thickness (h_u), however, decreased with increasing cutting speed. Thus, the saw teeth tend to get more pronounced with increased feed rate. The undeformed surface width in the segmented chip tended

to increase linearly with the feed rate increase but was seemingly less affected by the cutting speed.

Results presented in Figure 6 (plot of the specific cutting energy - SE, total machining energy - ETME and actual cutting energy – EACU, as function of material removal rate) clearly illustrates that as the rate of material removal increases, the specific cutting energy required to produce a unit quantity of chip (unit volume of material) decrease. The lowest specific cutting energy occurs about the highest material removal rate and vice versa. This is partly the result of the actual cutting mechanism and the energy use of the ancillary equipment of the machine tool. At high material removal rates heat conduction in the cutting zone is reduced and the essentially constant cooling arrangement (flood cooling in this case) becomes less effective. This implies higher temperatures in the cutting zone and a more effective adiabatic shear zone due to increased softening of the workpiece material in the cutting zone during the upliftment phase of the segmentation process. The plastic instability that then forms produces shear and segmentation results. The significant strain developed in the segmented chip shear bands give effect to the rise in temperatures in the higher hardness material, and at elevated cutting speed this results in high-speed slip of the shear bands to occur much easier along the subsisting micro-cracks.

The gradient of segmentation plot, presented in Figure 7, shows that larger gradients (longer shear movements) occurs at the higher material removal rates or the lowest specific energies. Therefore, higher material removal rates imply less effective heat conduction leading to higher temperature and more energetic shear zone that then shears for an extended distance. The results plot, in Figure 7, further shows that specific cutting energy decreases with increasing gradient of segmentation upto a deepest trough point beyond which the specific cutting energy tends to increase again. This suggests the existence on an optimal chip gradient of segmentation point at which the specific cutting energy used will be minimum. The

Table: 2 Experiment Results Summarised

| Cutting speed, m/min | Feed rate, mm/rev | Total machining energy, J | Specific cutting energy, J/mm ³ | Chip width μm | Teeth pitch μm | San (θ) | Deg. Seg. | Seg. Freq, Htz |
|----------------------|-------------------|---------------------------|--|--------------------------|---------------------------|------------------|-----------|----------------|
| 50 | 0.1 | 587864 | 2408.22 | 141.33 | 51.06 | 65.55 | 0.63 | 16320.67 |
| 50 | 0.2 | 404186.5 | 1214.88 | 222.01 | 90.56 | 61.32 | 0.87 | 9202.00 |
| 50 | 0.3 | 258026 | 628.42 | 291.18 | 148.73 | 53.88 | 0.76 | 5603.12 |
| 70 | 0.1 | 523725 | 2120.16 | 108.47 | 45.73 | 57.89 | 0.85 | 25513.92 |
| 70 | 0.2 | 216690.5 | 660.71 | 217.33 | 113.77 | 65.52 | 1.19 | 10254.91 |
| 70 | 0.3 | 170905 | 405.28 | 295.50 | 161.87 | 49.65 | 0.67 | 7207.58 |
| 100 | 0.1 | 342060 | 1355.13 | 119.23 | 59.74 | 57.12 | 0.66 | 19643.28 |
| 100 | 0.2 | 164690 | 407.15 | 234.50 | 88.79 | 49.91 | 1.01 | 18770.18 |
| 100 | 0.3 | 194029 | 276.54 | 291.57 | 153.73 | 54.85 | 0.92 | 10841.28 |
| 150 | 0.1 | 338654 | 778.38 | 109.95 | 47.42 | 49.69 | 0.98 | 35796.00 |
| 150 | 0.2 | 184528 | 261.244 | 206.93 | 123.43 | 53.77 | 0.75 | 20253.85 |
| 150 | 0.3 | 134207.5 | 173.20 | 438.97 | 159.37 | 45.79 | 1.09 | 15687.09 |
| 200 | 0.1 | 244882.5 | 459.01 | 130.00 | 79.57 | 45.32 | 0.52 | 41893.59 |
| 200 | 0.2 | 138382.5 | 174.68 | 184.53 | 123.07 | 53.75 | 0.69 | 27085.59 |
| 200 | 0.3 | 96909.5 | 90.04 | 231.83 | 159.13 | 48.47 | 0.67 | 20946.80 |
| 250 | 0.1 | 210571.5 | 388.20 | 155.90 | 71.29 | 46.77 | 0.51 | 47894.00 |
| 250 | 0.2 | 208470.5 | 184.71 | 184.57 | 126.83 | 45.69 | 0.70 | 32851.51 |
| 250 | 0.3 | 150674.5 | 161.19 | 236.40 | 161.48 | 37.62 | 0.84 | 31304.78 |

Key: Seg. Freq. - segmentation frequency; San - Segmentation angle; Deg. Seg. - Degree of segmentation

Table 3: Chip morphology results – changing cutting speed at constant feed rate


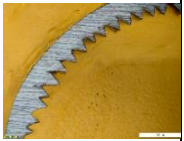
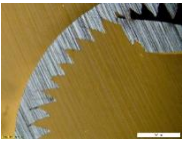
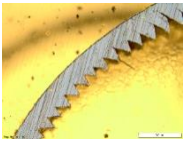
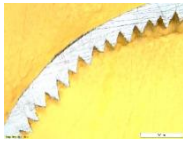
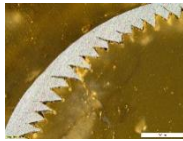
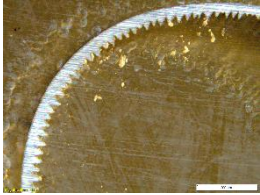
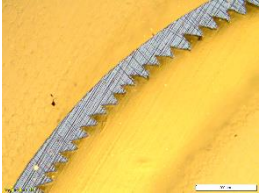
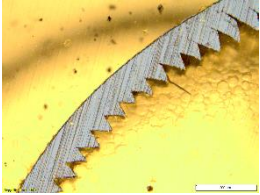
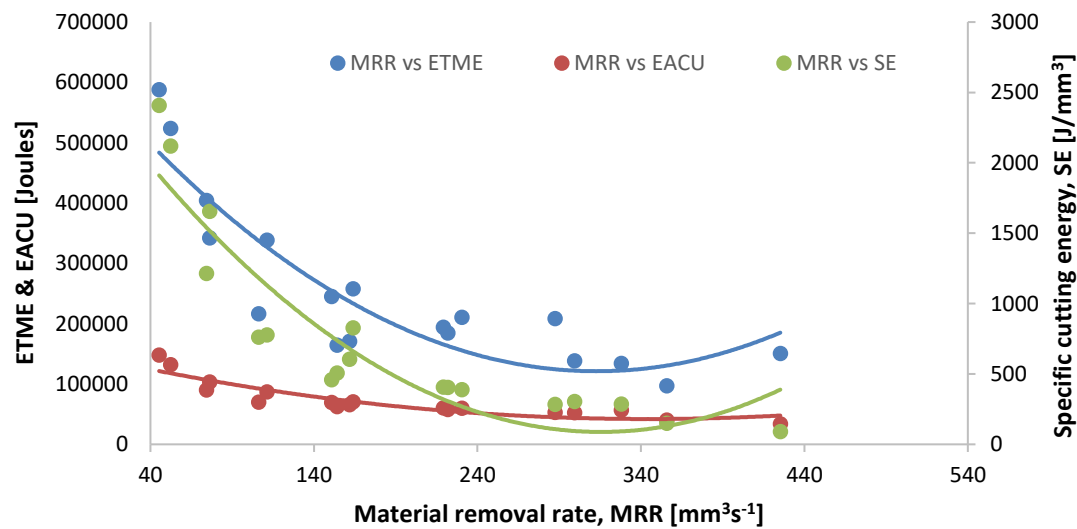
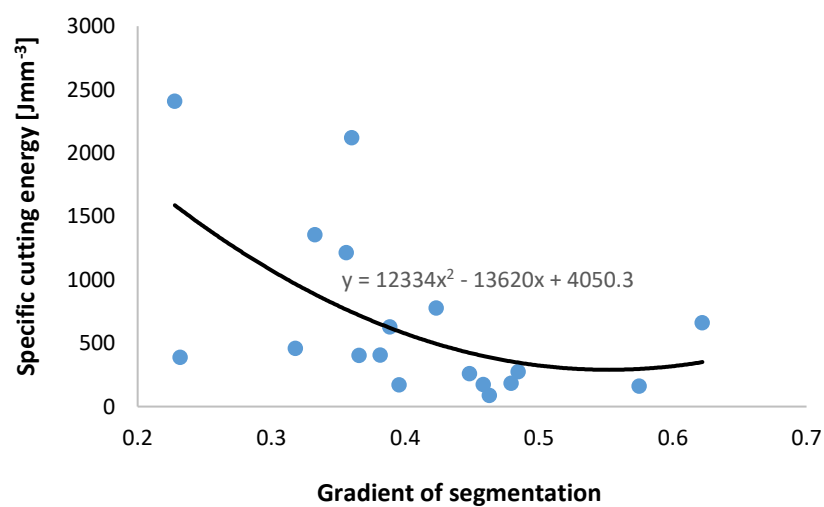
| | 50 m/min | 70 m/min | 100 m/min | 150 m/min | 200 m/min | 250 m/min |
|------------|---|---|---|--|---|---|
| 0.3 mm/rev |  |  |  |  |  |  |
| | $EACU = 70484 \text{ J}$ $\text{Energy } \eta = 22.21\%$ | $EACU = 65550 \text{ J}$ $\text{Energy } \eta = 24.12\%$ | $EACU = 60618 \text{ J}$ $\text{Energy } \eta = 35.66\%$ | $EACU = 56808 \text{ J}$ $\text{Energy } \eta = 43.42\%$ | $EACU = 40117 \text{ J}$ $\text{Energy } \eta = 42.13\%$ | $EACU = 33730 \text{ J}$ $\text{Energy } \eta = 46.71\%$ |

Table 4: Chip morphology results – changing feed rate at constant cutting speed

| | 0.1 mm/rev | 0.2 mm/rev | 0.3 mm/rev |
|-----------|---|--|---|
| 150 m/min |  |  |  |
| | $EACU = 86699 \text{ J}$ $\text{Energy } \eta = 26.54\%$ | $EACU = 57970 \text{ J}$ $\text{Energy } \eta = 34.28\%$ | $EACU = 56808 \text{ J}$ $\text{Energy } \eta = 43.42\%$ |

**Figure 6: Material removal rate, MRR vs specific cutting energy, SE****Figure 7: Variation of specific cutting energy as a function of gradient of segmentation**

gradient of segmentation is closely related to the specific cutting energy, thus, and it shows that the larger gradients (longer shear movements) occur at the higher material removal rates or the lowest specific energies. Therefore, higher material removal rates imply less effective heat conduction leading to higher temperature and more energetic shear zone that then shears for an extended distance. This emanates from the higher temperatures experienced in the cutting zone wherein a more effective adiabatic shear zone, due to increased softening of the workpiece material in the cutting zone, exist during the upliftment phase of the segmentation process. The plastic instability that then forms produces shear and segmentation results.

Chip segmentation frequency - which is an aspect of the mechanism of shear localisation – represents the number of chip segments produced per given unit length or time, is indirectly related with the specific cutting energy (Figure 8) and material removal rates by the process of high performance cutting and high speed machining respectively. Chip segmentation frequency was considered, in the present work, due to its direct and indirect effects on the cutting forces, chattering, process smoothness, residual stress pattern and intensity, (Mabrouki, et al., 2008) and inadvertently, the energy use efficiency.

The Shear angle parameter determination is of fundamental significance in understanding chip formation during the metal machining process. The results of shear angle versus specific cutting energy are presented in Figure 9, where it is apparent that lower chip segmentation angle is associated with higher specific cutting energy use. Smaller shear segmentation angles are associated with higher cutting shear strain, larger cutting forces and higher cutting power requirements. The same is true with the higher shear segmentation angles beyond the optimum shear segmentation angle. The larger the shear segmentation angle imply less shear plane area and less chip thickness which in itself lead to the experiencing of less cutting forces, due to temperature elevation in the cutting zone,

less shear strain and higher power requirement of the material separation process and costly tool wear due to the high thermal exposure. On the other hand, less chip thickness threatens tool life and workpiece material surface integrity, due to inadequate heat conduction surface from the cutting zone.

Average chip thickness was derived from taking three measurements each, respectively, of maximum thickness and minimum thickness, sum them up and then dividing by three in order to arrive at the average chip thickness. This parameter is useful in projecting the chip ratio as well as obtaining the segmentation frequency of the chip. The results of chip segmentation pitch, as it influences the specific cutting energy, are presented in Figure 10. It is apparent that chip chip segmentation pitch increases as the specific cutting energy decreases towards an optimum chip thickness point, beyond which the specific cutting energy seems to rise again.

The results of Specific cutting energy as a function of chip thickness, plot, is presented in Figure 11. The character of the plotted curve is such that specific cutting energy consumption decreases with the increase in the segmentation teeth pitch up to some point beyond which the specific cutting energy tends to increase again. Attaining an energy efficient average chip thickness for the particular machining operation would be a helpful intention of the machining process planning.

The ratio of the chip material thickness before cutting to the thickness of the chip material thickness after cutting is referred to as the chip compression ratio or the chip thickness ratio. This derives from the similarity of the volume of the material before and after cutting – implying that the volume of the material removed is equal to the volume of the chip material. Chip compression ratio is an essential attribute in describing the effect of the machine operating parameters on the morphology of the chip (Shaw, 1997). The results plot, in Figure 12, shows the proportionate reduction of the specific cutting energy with an increase in the chip compression ratio.

The interaction curve between the chip ratio and the specific cutting energy suggest the existence of an optimum chip compression ratio point at which the specific cutting energy gets to be at its

minimum most and beyond which point the specific cutting energy tend to increase again with continued increase in the chip ratio.

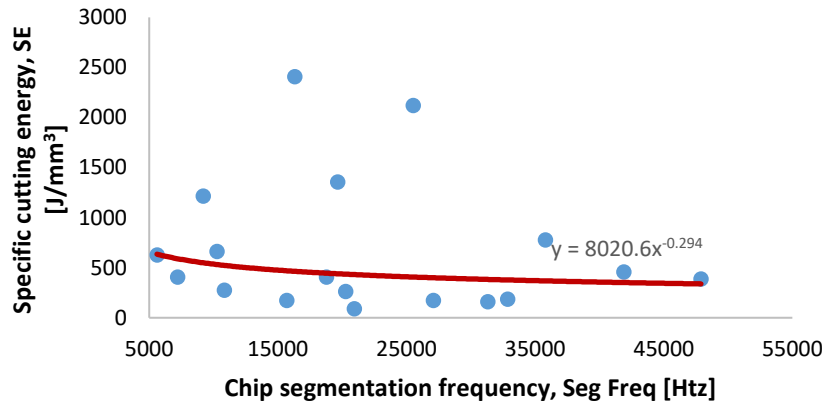


Figure 8: Variation of specific cutting energy with change in chip shear segmentation frequency

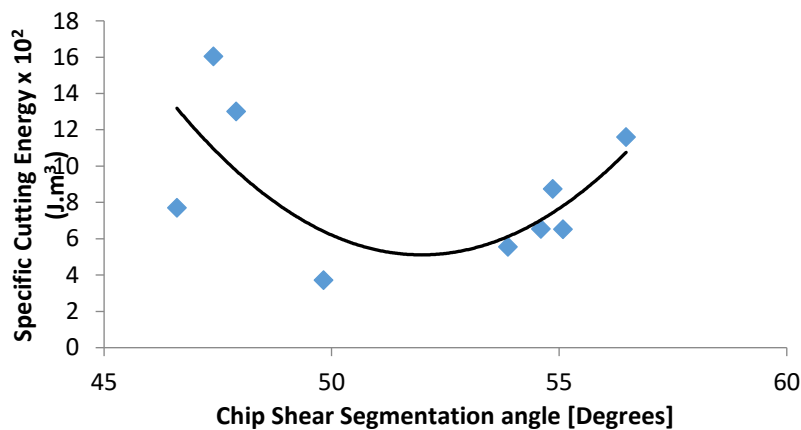


Figure 9: Variation of specific cutting energy as a function of chip shear segmentation angle

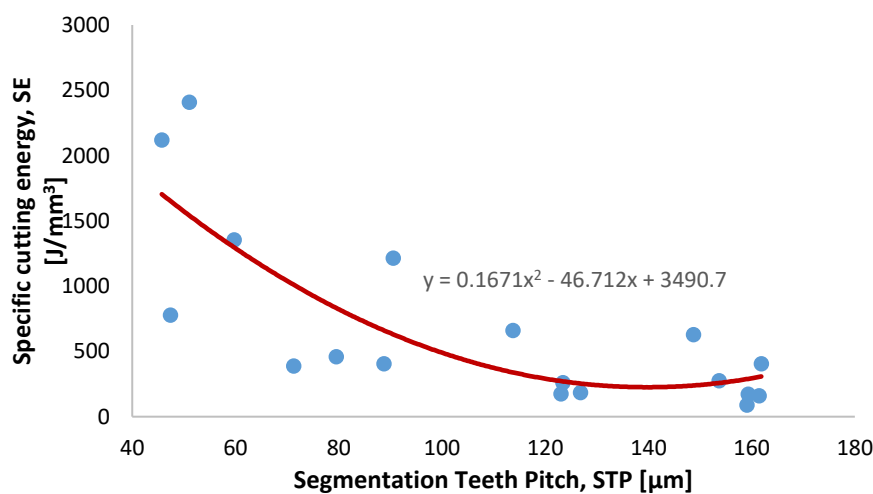


Figure 10: Variation of specific cutting energy as a function of chip shear segmentation pitch

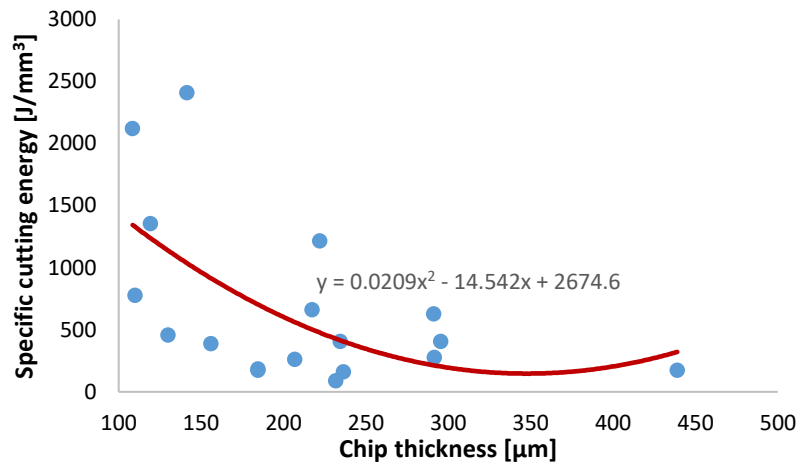


Figure 11: Variation of specific cutting energy as a function of chip thickness

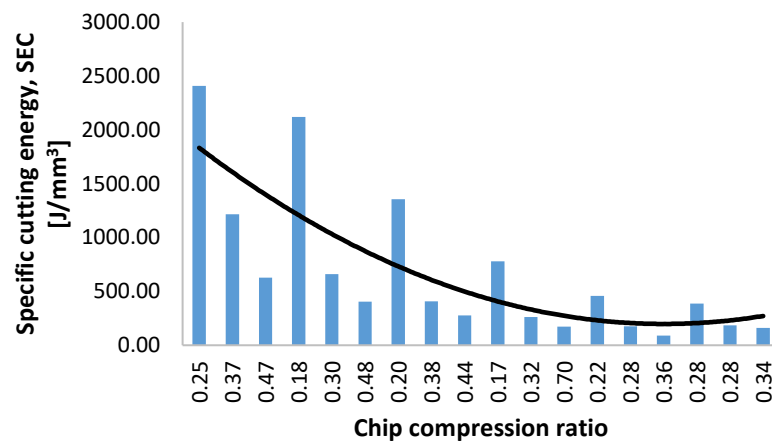


Figure 12: Variation of specific cutting energy as a function of chip compression ratio

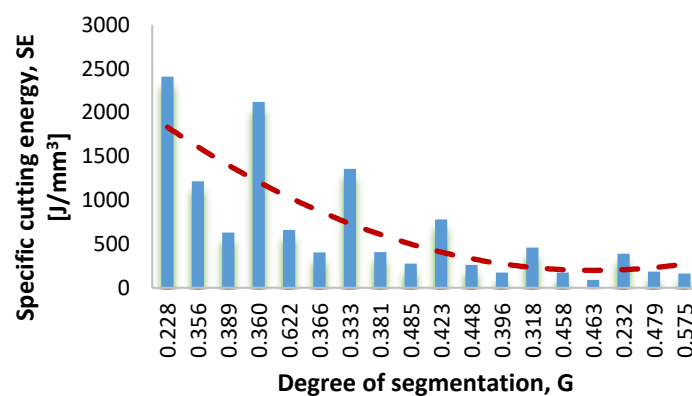


Figure 13: Variation of specific cutting energy as a function of degree of segmentation

4. CONCLUSIONS

Research results presented, in this study, are of interest and provide significant insight, into machining science and related phenomena, to machining-based production engineers, machining process operatives and process planners. This perspective enhance machining productivity through optimum parameter selection, particularly energy use at the machining process level. Earlier studies had established that the effect of the cutting conditions on the machining process derive significantly from the chip segmentation mechanism (Mason, et al., 2011). A study on the Effect of chip morphology on specific energy use, for the purpose of extracting the data such that the link between chip morphology and specific cutting energy - independent from the change in cutting parameters – was conducted in this current work. The research studied and characterised chip morphology features – inter alia: segmentation spacing (teeth segmentation pitch), degree of segmentation, chip deformation coefficient, shear segmentation angle, chip segmentation frequency – through experimental investigation. Ensuing are the significant conclusions deriving from the present work. The experimental study results established new insights into the chip morphology profile parameters and specific energy use relationships. The most ineffective use of energy occurs at low level chip morphology parameter combinations for all the considered features, except the variation of specific cutting energy as a function of chip shear segmentation angle where ineffectiveness was apparent at both lower and higher segmentation angle beyond the optimal chip segmentation angle size. This is due to the increased mechanical and thermal load which occur in the cutting zone, at the low operating parameter level. Thus, in order to reduce energy consumption of the machining process it is essential to operate in the high chip morphology parameter generating range.

Overall, the most effective energy use occurs at high material removal rate, which implies the use of high cutting speeds and

high feed rates (Oosthuizen, et al., 2013). Energy use decreases (pointing towards possibly large energy savings) with increased feed rate and cutting speed, as shown on the material removal rate and energy plot cluster curves. Increased material removal rate is also inadvertently linked with increased feature parameter sizes in the morphology of the segmented chip generated. Observably, the chip segmentation formation will be transiting also as the cutting conditions are adjusted. As the cutting speed or feed rate increases, the temperature of the cutting process increases. This renders the resistance to plastic deformation, of the material, to decrease. The metal starts deforming, plastically, when the applied stress reaches the level of flow stress - as it is mostly influenced by temperature, strain, strain rate and material properties. The average flow stress in a shear band along the length of the new shear decrease with increasing cutting condition such as cutting speed. This is consistent with changes in the feature parameter sizes of the chip morphology, as presented in the results above in section 4. Thus, it is feasible to monitor the energy consumption of the machining process indirectly by observing the chip system once a determinate optimum point had been established. It can be concluded, from the experiment results, that an understanding of the chip morphology characterisation, with the specific cutting energy of the machining process, gives indication of the material machinability. The observed changes in the chip morphology reflects the effective amount of the energy used during the cutting process. As such, therefore, the feasibility to monitoring the energy consumption of the machining process, by observing the chip system, had been established. Further work, relating to the current study, is concerned about determining the optimum cutting conditions for energy efficiency by making use of the chip formation models developed from the research.

5. ACKNOWLEDGEMENTS

The author would like to acknowledge the generous contribution of the University of

Johannesburg Advanced Manufacturing Research Centre for providing the experimental resources and testing facilities which were used in generating important data during the writer's PhD studies period at the university.

REFERENCES

- Diaz, N., Helu, M., Jarvis, A., Tonissen, S., Dornfeld, D., Schlosser, R., 2009. *Strategies for minimum energy operation for precision machining*, Laboratory for Manufacturing and Sustainability, UC Berkeley, <https://escholarship.org/uc/item/794866g5>.
- Anderberg, S., Beno, T. & Pejryd, L., 2012. Energy and Cost Efficiency in CNC Machining from a Process Planning Perspective. In: *Sustainable Manufacturing: Shaping Global Value Creation*, IX. Berlin: Springer Berlin Heidelberg, DOI 10.1007/978-3-642-27290-5_63, Print ISBN 978-3-642-27289-9, Online ISBN 978-3-642-27290-5, pp. 393-398.
- Annamarie, T., 2004. *Titanium alloy Guide*, Staffordshire: RMI Titanium Company.
- ASM International, 1988. *Titanium: A Technical Guide*. In: Ohio: ASM International, Materials Park, OH, 44073-0002, pp. 75-85.
- Astakhov, V. P. & Shvets, S., 2004. The Assessment of Plastic Deformation. *Journal of Materials Processing Technology*, Volume 146, pp. 193 - 202.
- Boyer, R. R., 1996. An overview on the use of titanium in the aerospace industry. *Materials Science and Engineering*, Volume 213A, p. 103-114.
- Calamaz, M., Coupard, D. & Girod, F., 2008. A new material model for 2D numerical simulation of serrated chip formation when machining titanium alloy Ti-6Al-4V. *International Journal of Machine Tools & Manufacture*, Volume 48, p. 275-288.
- Collogs, E. W., 1983. *The Physical Metallurgy of Titanium Alloys* (ed ASM). s.l.:ASM.
- Cook, N. H., 1953. *Chip formation in machining titanium*. Watertown Arsenal, s.n.
- Dabrowski, R., 2011. The Kinetics of Phase Transformations During Continuous Cooling of Ti6Al4V Alloy from the Diphase $\alpha + \beta$ Range. Volume 56 (217-221)(2).
- Dahmus, J. B. & Gutowski, T. G., 2004. *An Environmental analysis of machining*. s.l., s.n.
- Draganescu, F., Gheorghe, M. & Doicin, C. V., 2003. Models of machine tool efficiency and specific consumed energy. *Journal of Materials Processing Technology*, Volume 141, p. 9-15.
- Ezugwu, E. O., Bonney, J. & Yamane, Y., 2003. An overview of the Machinability of Aero engine Alloys. *Journal of Materials Processing Technology*, Volume 134, p. 233-253.
- Ezugwu, E. O. & Wang, Z. M., 1997. Titanium Alloys and their Machinability - a Review. *Journal of Materials Processing and Technology* 68, pp. 262-274.
- Guo, Y., Loenders, J., Dufloy, J. & Lauwers, B., 2012. Optimisation of Energy Consumption and surface quality in finish turning. *ScieVerse Science Direct Procedia CIRP*, Volume 1, pp. 512-517.
- Gutowski, T., Dahmus, J. & Thiriez, A., 2006. *Electrical Energy Requirements for Manufacturing Processes*. Leuven, s.n.
- Hou, Z. B. & Komanduri, R., 1995. On a Thermo-mechanical Model of Shear Instability in Machining. *CIRP Annals*, 44(1), p. 69-73.
- Hua, J. & Shivpuri, R., 2004. Prediction of chip morphology and segmentation during the machining of titanium alloys. *Journal of Materials Processing Technology*, Volume 150, p. 124-133.
- ISO 9000:200, 2000. *Quality Management Systems - Fundamentals and Vocabulary*, s.l.: International Standards organisation.
- Jawahir, I. S. et al., 2011. Surface Integrity in Material Removal Processes: Recent Advances. *CIRP Annals - Manufacturing Technology* 60(2), p. 603-626.
- Kalpajian, S. & Schmidt, S. R., 2009. *Manufacturing Engineering and Technology*, Pearson Education.
- Liu, F., Wang, Q. & Liu, G. I., 2013. Content Architecture and Future Trends of Energy Efficiency Research on Machining Systems. *Chin J Mech Eng*, 49(19), pp. 87-94.
- Mabrouki, T., Girardin, F., Asad, M. & Rigal, J. F., 2008. Numerical and experimental study of dry cutting for an aeronautic aluminium alloy (A2024-T351). *International Journal of Machine Tools Manufacturing*, Volume 48, p. 187-197.
- Machado, A. R. & Wallbank, J., 1989. Machining of Titanium and its alloys - a review. *IMechE*, Volume 204, pp. 53-60.
- Ma, J., Ge, X., Chang, S. I. & Lei, S., 2014. Assessment of Cutting Energy Consumption and Energy Efficiency in Machining of 4140 Steel. *International Journal of Advanced Manufacturing Technology*, Volume 74, pp. 1701-1708.
- Mason, D. M., Yong, H. & Jian, L., 2011. Chip Morphology Characterisation and Modeling In Machining Hardened 52100 Steels. *Machining Science and Technology: An International Journal*, 11(3), pp. 335-354.
- Miroslav, N., Ivan, M., Robert, C. & Mária, C., 2013. Influence of Cutting Speed on Intensity of the Plastic Deformation During Hard Cutting. *Materials and Technology*, Volume 47, p. 745-755.
- Neugebauer, R., Schubert, A., Reichmann, B. & Dix, M., 2011. Influence exerted by tool properties on the energy efficiency during drilling and turning operation. *CIRP Journal of Manufacturing Science and Technology*, Volume 4, p. 161-169.
- Oosthuizen, G. A., Laubscher, R. F., Tayisepi, N. & Mulumba, J. K., 2013. *Towards Energy Management during the Machining of Titanium Alloys*. Stellenbosch, s.n.
- Oosthuizen, G. A., Akdogan, G., Dimitrov, D. & Treurnicht, N. F., 2010. A Review of the Machinability of Titanium Alloys. *Research and Development Journal of the South African Institution of Mechanical Engineering* 26, pp. 43-52.
- Ozel, T. & Ulutan, D., 2012. Prediction of machining induced residual stresses in turning of turning of titanium and nickel based alloys with experiments and finite element simulations. *CIRP Annals - Manufacturing Technology*, Volume 61, p. 547-550.
- Paul, H. C., 2007. *ASM Handbook Volume 16 - Machining*, s.l.: The Pennsylvania State University.
- Rajemi, M. F. & Mativenga, P. T., 2008. Machinability Analysis from Energy Footprint Considerations. *Journal of Machine Engineering* 8 (2);, pp. 106 - 13.

- Rajemi, M. F., Mativenga, P. T. & Jaffery, S. I., 2009. Energy and carbon footprint analysis for machining titanium Ti-6Al-4V Alloy. *Journal of Machine Engineering*, 9(1), p. 103–112.
- Repro, 2002. *Sandvik 40857-C-2920-18, C-2920-18-ENG-043-074*, Stockholm: Sandvik Coromant.
- Ribeiro, M. V., Moreira, M. R. V. & Ferreira, J. R., 2003. Optimization of titanium alloy (6Al-4V) machining. *Journal of Materials Processing Technology*, Volume 143-144, pp. 458-463.
- Sebastian, T., 2012. *Energy Efficiency in Manufacturing Systems*. Germany: Springer.
- Shaw, M. C., 1997. *Metal Cutting Principles*. Oxford: Clarendon Press.
- Sun, J. & Guo, Y. B., 2008. A new multi-view approach to characterize 3D chip morphology and properties in end milling titanium Ti- 6Al- 4V. *International Journal of Machine Tools & Manufacture*, Volume 48, p. 1486– 1494.
- Tao, V. P. & Xun, X., 2013. A Universal Hybrid Energy Consumption Model for CNC Machining Systems. In: *Re-Engineering Manufacturing for Sustainability: Proceedings of the 20th CIRP International Conference on Life Cycle Engineering, Singapore, 17-19 April 2013*. Singapore: Springer Singapore, pp. 251-256.
- Tayisepi, N., Laubscher, R. F. & Oosthuizen, G., 2016. *Energy Efficiency and Surface Integrity Assessment During the Machining of Titanium Alloys*. Stellenbosch, South Africa, Proceedings of COMA'16.
- Upadhyay, V., Jain, P. K. & Mehta, N. K., 2014. *Comprehensive Study of Chip Morphology in Turning of Ti-6Al-4V*. IIT, Guwahati, Assam, India, s.n.
- Vyas, A. & Shaw, M. C., 1999. Mechanics of saw-tooth chip formation in metal cutting. *Journal of Manufacturing Science and Engineering*, 121(2), p. 163–77.
- Vyas, A. & Shaw, M. C., 1999. Mechanics of saw-tooth chip formation in metal cutting. *Journal of Manufacturing Science and Engineering*, 121(2), p. 163–17.
- Vyas, A. & Shaw, M. C., 1999. Mechanics of Saw-Tooth Chip Formation in Metal Cutting. *Journal of Manufacturing Science and Engineering*, Volume 121, pp. 163-172.
- Zhou, L. et al., 2016. Energy Consumption Model and Energy Efficiency of Machine Tools: A Comprehensive Literature Review. *Journal of cleaner production*, Volume 112, pp. 3721-3734.